## RESEARCH PAPER

# First-Principles Analysis of Cr-Doped SrTiO<sub>3</sub> Perovskite as Optoelectronic Materials

Hussein A. Miran<sup>1,\*</sup>, Zainab N. Jaf<sup>1</sup>, Mohammednoor Al Tarawneh<sup>2</sup>, M Mahbubur Rahman<sup>3</sup>, Auday Tariq Al-Bayati<sup>1</sup>, Ebtisam M-T. Salman<sup>1</sup>

Received: October 2022 Revised: March 2023 Accepted: March 2023

DOI: 10.22068/ijmse.3028

**Abstract:** The influence of  $Cr^{3+}$  doping on the ground state properties of  $SrTiO_3$  perovskite was evaluated using GGA-PBE approximation. Computational modeling results infered an agreement with the previously published literature. The modification of electronic structure and optical properties due to  $Cr^{3+}$  introducing into  $SrTiO_3$  were investigated. Structural parameters assumed that  $Cr^{3+}$  doping alters the electronic structures of  $SrTiO_3$  by shifting the conduction band through lower energies for the Sr and Sr is sesides, results showed that the band gap was reduced by approximately 50% when presenting one  $Sr^{3+}$  atom into the  $SrTiO_3$  system and particularly positioned at Sr sites. Interestingly, substituting Sr is it by  $Sr^{3+}$  led to eliminating the band gap indicated a new electrical case of transferring semiconducting material into a conducting material which intern enhance conductivity. Furthermore, it was found that  $Sr^{3+}$  doping either at Sr or  $Sr^{3+}$  positions could effectively develop the  $Sr^{3+}$  dielectric constant properties. In addition, the absorption spectra was extended to cover the visible light region of the electromagnetic radiation, indicating the capability of this compound in harvesting sunlight for solar cell applications. Consequently, it can be said that  $Sr^{3+}$  is an effective dopant which opening up new prospects for various industrial and technological applications.

**Keywords:** Perovskite oxide-lead-free ceramics,  $Cr^{3+}$  metal doping, Band gap, Elastic constants, First-principles calculations, Optoelectronics.

#### 1. INTRODUCTION

Strontium titanate (SrTiO<sub>3</sub>) as lead-free ceramic is one of the perovskite oxide materials that are characterized with the stoichiometric of ABO<sub>3</sub> with high melting point of 2080°C. This type of materials exhibits significant characteristics [1-3]. These span a range of expedient applications for instance, in the field of microelectronics, SrTiO<sub>3</sub> thin films have widely been employed owing to their high dielectric constant, which promote their use as an insulating layer in integration circuits. Furthermore, due to the close lattice matches with several superconducting materials, SrTiO<sub>3</sub> has been considered as an epitaxial insulating layer in high Tc thin-film multilayers [4]. The wide band gap of SrTiO<sub>3</sub> (~3.2 eV) indicates that only a trivial part of ultra violet region (UV) can be absorbed which limits photocatalytic performance. modifying the electronic structure of the host system (i.e., SrTiO<sub>3</sub>) by doping with various metal

and non-metal elements can narrow the band gap which in turn shift the optical absorption edge from the UV to the visible light region [5]. A study has demonstrated that an enhancement in the photocatalytic property of SrTiO<sub>3</sub> can be attained by incorporating noble metal ions (Mn, Ru, Rh, and Ir) [6]. Heavy elements such as La and Nb have experimentally been loaded into SrTiO<sub>3</sub> system [7]. Results showed that altering the doping levels of La and Nb would result in reducing the thermal conductivity of 1.97 W m<sup>-1</sup> K<sup>-1</sup>. It has also been reported that loading La into Ir-doped SrTiO<sub>3</sub> can effectively improve the photocatalytic performance under UV spectrum Mei al.fabricated a novel [8]. et perovskite/carbon nitride heterojunction  $(SrTiO_3/g-C_3N_4)$ to be utilized photocatalytic reduction of U(VI). Their findings demonstrate that perovskite-based composites can be applied in the actual environmental cleanup under visible-light to improve solar energy utilization [9]. UV-vis analysis of the



<sup>\*</sup> hussein.a.j@ihcoedu.uobaghdad.edu.iq

<sup>&</sup>lt;sup>1</sup> Department of Physics, College of Education for Pure Sciences - Ibn Al-Haitham, University of Baghdad, 10071 Baghdad, Iraq

<sup>&</sup>lt;sup>2</sup> Department of Chemical and Petroleum Engineering, United Arab Emirates University, Sheikh Khalifa bin Zayed Street, Al-Ain 15551, United Arab Emirates

<sup>&</sup>lt;sup>3</sup> Department of Physics, Jahangirnagar University, Savar, Dhaka 1342, Bangladesh

synthesized SrTi<sub>1-x</sub>Cr<sub>x</sub>O<sub>3</sub> powders revealed that the absorption spectra is extended to include UV and visible-light spectrum, while loading Chromium dopants at x = 0.00, 0.02, 0.05, 0.10SrTiO<sub>3</sub> by replacing Ti sites [10]. Furthermore, using the polymeric precursor procedure, SrTiO<sub>3</sub> and Cr-doped SrTiO<sub>3</sub> SrTi<sub>1-x</sub>Cr<sub>x</sub>O<sub>3</sub> has been fabricated at low temperature of about 450°C. Results showed that new that when introducing Cr3+ into SrTiO3, a band gap in the visible light spectrum was generated [11]. The codoping of Cr, La with SrTiO<sub>3</sub> nanoparticles has been carried out by Tonda et al. [12]. Findings displayed that the band gap has been reduced from 3.2 eV in the UV spectrum for undoped system to 2.1 eV in the visible spectrum for Cr-codoped SrTiO<sub>3</sub>. However, they reported that an enhancement in the photocatalytic activity of Cr,La-codoped SrTiO<sub>3</sub> nanoparticles by diminishing the band gap up to 1.9 eV under sunlight radiation.

On the other hand, great deal of efforts has been first-principles dedicated on calculations represented by density functional theory (DFT) to provide an insight into the ground state properties of various metal oxides systems, involving, structural, electronic, optical, and mechanical properties [13–15]. Particularly, perovskite oxides are well investigated by DFT study that has revealed that introducing metal atoms such as, K and Na at Sr site into SrTiO<sub>3</sub> system would be employed as a p-type electrodes for solid-oxide fuel cell (SOFC) industry [16]. First-principles calculations have been also performed on Crdoped SrTiO<sub>3</sub> to assess the consequence of Crdoping on the band gap states and the photocatalytic activity of SrTiO<sub>3</sub>. Besides, to evaluate the energy required for Cr-doping, the defect formation energy is calculated. Results showed that substituting Cr for Sr site necessitates slighter formation energy than substituting Cr for Ti in the Cr-doped SrTiO<sub>3</sub>. Particularly, Cr-doped SrTiO<sub>3</sub> can absorb visible light and its photocatalytic activity improved with rising Cr<sup>3+</sup> dopant contents [17]. The correlation between the oxidation state of Cr and photocatalytic performance has theoretically been investigated. The results demonstrated that the Cr<sup>3+</sup> is preferably located at the Ti site which exhibits a crucial role in visible-light absorption and the improvement of photocatalytic activities of Crdoped SrTiO<sub>3</sub> [18]. A DFT investigation

performed to assess the influence of Ag additive on SrTiO<sub>3</sub>. An improvement in the absorption spectra has been detected when introducing Ag into the SrTiO<sub>3</sub> system. Additionally, several results has been reported in that the energy band gap has been narrowed by 0.15 eV, the indirect band gap has been changed into direct band gap with converting the system from an n-type to a p-type semiconductor [19]. Zhou *et al.* [20] reported that adding rare earth elements (Pr, Nd, and Sm) would enhance the mechanical and dielectric properties of the strontium titanate.

To this end, the present contribution investigates the electronic and optical properties of SrTiO<sub>3</sub> perovskite under the framework of density functional theory calculations. Furthermore and for the first time the influence of substituting Sr and Ti atoms by chromium (Cr<sup>3+</sup>) at two different dopant concentrations of (0.125 and 0.250) on the optical properties (reflectivity, absorption, dielectric function, and conductivity) of the resultant configuration was extensively studied and represents the novelty of this study. In addition, charge distribution and formation energy have also been reported. The improvement in the optical properties is ascribed to the insertion of Cr3+ which stimulates various optoelectronic fields.

# 2. EXPERIMANTAL PROCEDURES

## 2.1. Computational Approach

In this investigation, Cambridge Serial Total Energy Package (CASTEP) software was implemented to study the electronic, structural and optical properties of Cr-doped SrTiO<sub>3</sub>. A super cell of  $2 \times 2 \times 2$  (40-atom/ 8-Sr, 8-Ti, and 24-O) has been constructed from the original optimized unit cell then optimization process to achieve the lowest energy configurations has been carried out. In the optimization criteria, Generalized Gradient Approximation (GGA) reported by Perdew Burke and Ernzerhof (PBE) (GGA-PBE) has been utilized for the considered arrangements [21]. The cut-off energy was fixed at 370 eV. Energy tolerance convergence was set at  $5 \times 10^{-6}$  eV/atom and in the Brillouin zone a kpoints of  $3 \times 3 \times 3$  as a Monkhorst-Pack grid was deployed [22] [23]. Ultrasoft pseudopotentials was chosen in the calculations. The valence electron configurations for Sr, Ti, Cr, and O, imply to [Kr]  $5s^2$ , [Ar]  $3d^2 4s^2$ ,  $3d^5 4s^1$ , and  $2s^2$ 



 $2p^4$ , respectively. The maximum displacement accuracy corresponds to  $1 \times 10^{-3}$  Å. The max stress tolerance corresponds to 0.05 GPa. To imitate the experimentally measured band gap of pure SrTiO<sub>3</sub> perovskite, scissor operator [24] was fixed at 1.37 eV. Finally, to evaluate the stability of the selected configurations, the defect formation energy ( $E_f$ ) has been considered using the following expression;

$$E_{Sr_kTi_lCr_nO_m} = \frac{1}{k+l+n+m} (E_{Sr_kTi_lCr_nO_m} - k \times E_{Sr} - l \times E_{Ti} - nE_{Cr} - m \times E_0)$$
 (1)  
Where the constants  $k$ ,  $l$ ,  $n$  and  $m$ , denote the molar fractions of elements Sr, Ti, Cr, and O correspondingly. The replacement steps were fulfilled at  $x = 0.125$ , and  $0.250$ . This infers that at  $x = 0.125$ , only single Sr atom has been replaced by  $Cr^{3+}$  while at  $x = 0.250$ , two Sr atoms have been exchanged by  $Cr^{3+}$ . Following the same procedure and content, Cr atoms were positioned at Ti sites.

#### 3. RESULTS AND DISCUSSION

# 3.1. Structural Relaxation and Analysis

For the conventional unit cell of SrTiO<sub>3</sub>, the atomic positions of Sr, Ti, and O correspond to (0,

0, 0), (0.5, 0.5, 0.5) and (0.5, 0, 0.5), respectively. Sr and Ti cations ensure considerably varied sizes where Sr exhibits higher atomic radius than Ti. The Sr and Ti cations accommodate the corner and the center of the cube, correspondingly, and the oxygen anions are positioned at the center of the cube edges.

The constructed  $2 \times 2 \times 2$  configurations are shown in Figures 1-2(a-d) which is ordered according to the chromium atom's contents and positions. The crystal structure of perovskite  $SrTiO_3$  reveals cubic unit cell with Pm3m space group [25]. The structural and electronic properties are documented in Table 1. The lattice parameters of the studied systems displayed in the table agreed with the published literature demonstrating that the considered model can reproduce the structural properties of  $SrTiO_3$  [26–28].

# 3.2. Electronic Modification Analysis

Generally, the perovskite oxides exhibit significantly ionic bonding character in addition to covalent nature. The ionic radius of Sr, Ti, and Cr refer to 1.44 Å, 0.605 Å, and 0.615 Å, respectively.

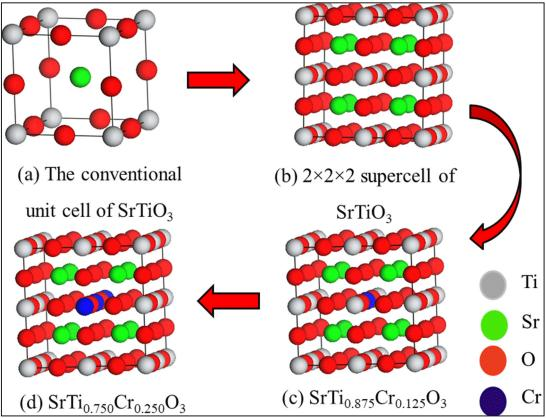


Fig. 1. The crystal structure of pure and Cr-doped perovskite SrTiO<sub>3</sub> configurations.



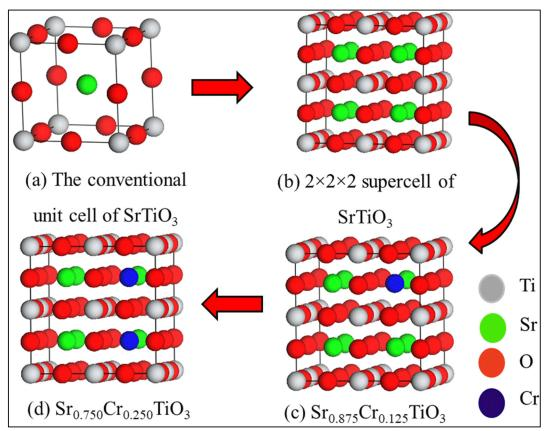


Fig. 2. The crystal structure of pure and Cr-doped perovskite SrTiO<sub>3</sub> configurations.

**Table 1.** The optimized lattice parameters (Å), band gap energy (eV), and charge distribution (e) for pure and Cr-loaded SrTiO3 configurations.

	Loading,	Lattice	Formation	Band gap	Charge distribution (e)			
Geometry		parameters (Å)	Energy (eV)	energy (eV)	Sr	Ti	Cr	О
Undoped SrTiO <sub>3</sub>	0	Present 3.94 Exp. 3.90 [27] Cal. 3.94 [26]	_	3.20 Exp. 3.25 [28] Cal. 3.57 [26]	1.38	0.85	-	-0.74
SrTi <sub>1-x</sub> Cr <sub>x</sub> O <sub>3</sub>	0.125	a=3.94	-7.96	0.00	1.39	0.825	0.53	-0.73
SrTi <sub>1-x</sub> Cr <sub>x</sub> O <sub>3</sub>	0.250	a=3.93	-7.94	0.00	1.41	0.800	0.47	-0.70
Sr <sub>1-x</sub> Cr <sub>x</sub> TiO <sub>3</sub>	0.125	a=3.94	-7.97	1.61	1.385	0.87	0.92	-0.735
Sr <sub>1-x</sub> Cr <sub>x</sub> TiO <sub>3</sub>	0.250	a=3.93	-7.95	1.43	1.377	0.89	0.95	-0.757

Charge distribution on atoms of the molecules is an important electronic analysis as it provides information about chemical bonds between atoms in the molecule. Positive values of the cation charges in undoped and Cr<sup>3+</sup>-doped SrTiO<sub>3</sub> demonstrate a covalent trend between them, whereas negative values of O atoms reveals an ionic tendency between these anion atoms and the cations in the studied systems. Moreover, (Sr or Ti) atoms replaced by Cr exhibit loss of their charges. However, O atoms gain more charges magnitudes as cation sites engaged by Cr<sup>3+</sup>. To understand the influence of the Cr atom

incorporation at Ti and Sr sites on the electronic properties of SrTiO<sub>3</sub>, the total and partial density of states (DOSs) have been calculated for pure configuration as depicted in Figure 4. The plot displays that the valence band (VB) is mainly consists of the O-2p states whereas the conduction band (CB) is mostly occupied by 3d states. Figure 5 portrays the electronic DOSs for Cr-doped SrTiO<sub>3</sub> at Ti site. The energy band gap of the pure system which is amounted to 3.20 eV (Figure 4 and Table 1) has been canceled when Cr atoms introduced and occupied Ti position in the structure as Figure 5 displayed.



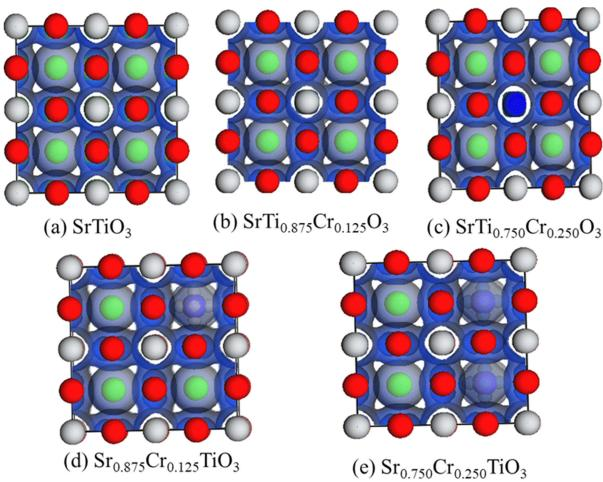
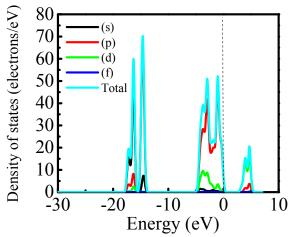


Fig. 3. Charge analysis of pure and Cr-doped SrTiO<sub>3</sub> configurations.

As a result, this work reports that Cr-doped SrTiO<sub>3</sub> at Ti sites with Cr<sup>3+</sup> atomic load of 0.125 and 0.250 demonstrate a conducting character.



**Fig. 4.** The total and partial density of states for pure SrTiO<sub>3</sub> system. The dashed line corresponds to the Fermi level.

Suggesting that the electronic band gap has been

canceled when Cr<sup>3+</sup> atoms were located at Ti bulk site shifting the material from semiconducting into conducting that exhibits metallic behavior as literature stated that Cr doping induces a transition from insulator/semiconductor to metal [29].

From other side, SrTiO<sub>3</sub> incorporated Cr at Sr sites remains as a semiconducting material but with less energy gap values tabulated in Table 1 and displayed in Figure 6. In addition, the calculated band gap energies correspond to 1.61 eV and 1.43 eV for the structure when Sr atomic locations being occupied by Cr<sup>3+</sup> atoms at atomic ratios of 0.125 and 0.250, respectively. Those band gaps are located in the range of visible wavelength.

# 3.3. Optical Characteristics

It is well known that for a material to be utilized in the optoelectronic and photovoltaic fields, optical behavior is crucial to provide an insight into its response to the incident electromagnetic radiation. This performance can be elucidated by



several wavelength dependent factors, terms as, reflectivity, absorption, the real  $\epsilon_1(\omega)$  and imaginary components  $\epsilon_2(\omega)$ , of the dielectric constants [30]. Initially, the optical properties of pure SrTiO<sub>3</sub> compound has been investigated then compared with the optical properties of Cr doped SrTiO<sub>3</sub> compound. The distortions displayed by perovskites as a result of cation replacement could be utilized to alter and modify properties of

attention including conductivity, dielectrics, etc. Variation of optical reflectivity with photon wavelength up to 800 nm is portrayed in Figure 7. Although the reflectivity spectra of pure and incorporated systems exhibit a moderate reflectivity values in ultra violet (UV) part of electromagnetic wavelength (EMW), they demonstrate small values in the visible part of EMW.

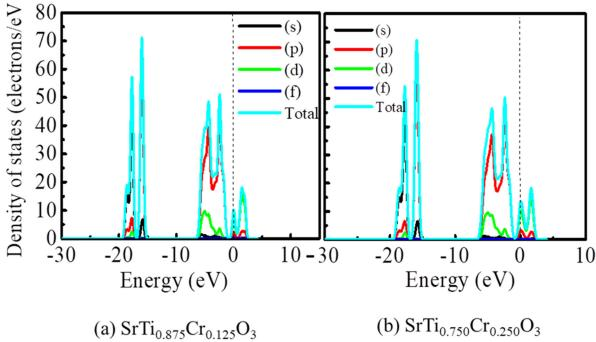


**Fig. 5.** The total and partial density of states Cr-doped SrTiO<sub>3</sub> at Ti sites. The dashed lines signify the Fermi level.

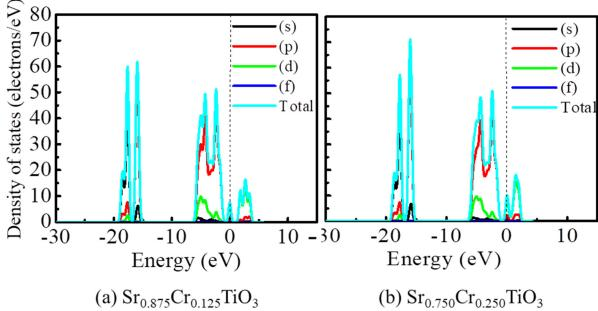
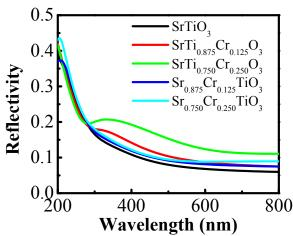


Fig. 6. The total and partial density of states Cr-doped SrTiO<sub>3</sub> at Sr sites. The dashed lines signify the Fermi level.





**Fig. 7.** The predicted reflectivity's of pure SrTiO<sub>3</sub> and Cr-doped SrTiO<sub>3</sub> structures.

Figure 8 shows the optical absorption coefficients of pure and doped SrTiO<sub>3</sub>. Pure SrTiO<sub>3</sub> reveals zero absorption values in the visible range. However, an enhancement in absorption property can be evidently seen in the visible range for the Cr–introduced SrTiO<sub>3</sub>, most notably for those configuration whose Ti sites were replaced by Cr<sup>3+</sup>.

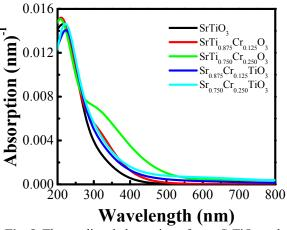


**Fig. 8.** The predicted absorption of pure SrTiO<sub>3</sub> and Cr-doped SrTiO<sub>3</sub> structures.

Furthermore, real part of complex dielectric constant is attained from Kramers–Kronig transformation. The real part of dielectric constant represents the polarizability of a material, whereas the imaginary part discloses the behavior of a material to be absorbing EMW incident on it and further reporting the regions of the sun rays at which the investigated material work as an absorber [31].

It can be obviously seen from Figures 9, 10 and

11 that dielectric constants, *i.e.*  $\epsilon_1(\omega)$  at zero energy, of the Cr-doped configurations have higher values in reference to the pure host system value. The rise of dielectric constant is also recorded as the portion of the Cr-dopant has been risen. However, a relatively observable increase in dielectric constant noticed with the configuration that Ti atoms replaced with  $Cr^{3+}$  contents of 0.250.

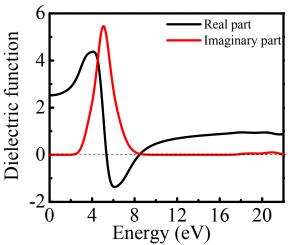


**Fig. 9.** The predicted dielectric function of pure SrTiO<sub>3</sub>.

It is critical to further evaluate the optical parameters of a material in order to render a benchmarking optical performance. One such parameter can be the optical conductivity that is an indication of transferring of the electronic charges through the optical object. As depicted in Figure 12, optical conductivity of the pure SrTiO<sub>3</sub> incurs zero values in the visible range, emphasizing the transparency trends as absorption spectrum.

Transparency property of SrTiO<sub>3</sub> in visible range of EMW can be deteriorated. Swapping Ti or Sr with Cr<sup>3+</sup> enhances the charge transfer occurrence of the host system in the visible region and stimulates the photovoltaic performance for the material to confidently be entering solar cell applications.

#### 3.4. Mechanical Properties

To examine the mechanical properties of bulk  $SrTiO_3$ , elastic constant  $(C_{ij})$ , bulk modulus (B), shear modulus (G), Young's modulus (E), Poisson's ratio (v), Zener anisotropy factor (A), and B/G ratio using both GGA-PBE and LDA functionals as revealed in Table 2.



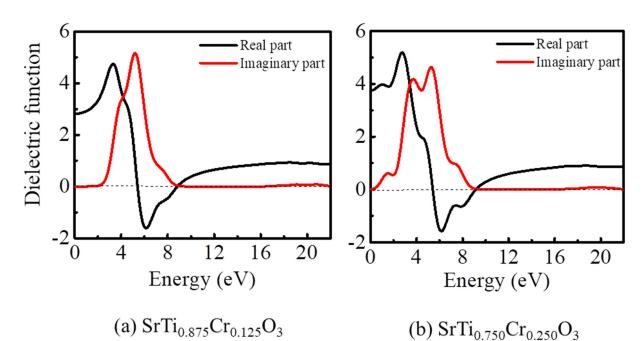


Fig. 10. The predicted dielectric function of Cr- SrTiO<sub>3</sub> at Ti sites.

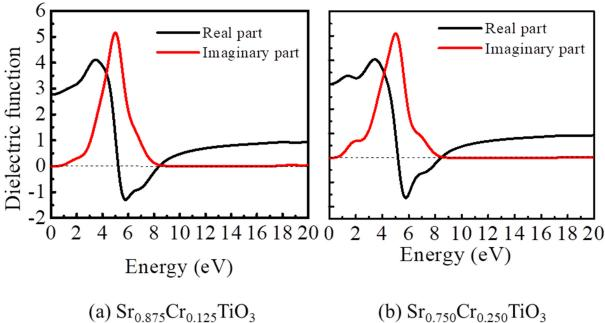


Fig. 11. The predicted dielectric function of Cr- SrTiO<sub>3</sub> at Sr sites.

**Table 2.** The elastic constants Cij (C11, C12, C44), bulk modulus (B), shear modulus (G), Young's modulus (E), Poisson's ratio (v), Zener anisotropy factor (A), and B/G ratio for the undoped SrTiO3 configuration.

						1				
Functional	C <sub>11</sub> (GPa)	C <sub>12</sub> (GPa)	C <sub>44</sub> (GPa)	B (GPa)	G (GPa)	E (GPa)	υ	A	B/G	
GGA-PBE	357.160	110.745	114.790	192.880	118.090	294.220	0.245	0.930	1.63	Present
LDA	331.710	95.205	112.590	174.040	114.820	282.370	0.230	0.950	1.51	study
GGA-PBEsol Exp.	350.46	101.16	111.02	184.26 178.8	116.28	288.22	0.24	0.89	1.58	Ref.[33] Ref.[37]



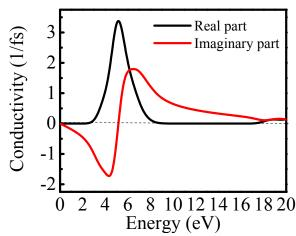


Fig. 12. The predicted conductivity of pure SrTiO<sub>3</sub>.

The elastic constant  $C_{11}$  describes the toughness of a material versus the resulted strains, C<sub>12</sub> implies the material shear stress, and C<sub>44</sub> demonstrates the resistance alongside shear distortion. First-principles calculations provide a comprehensive insight into the mechanical properties of cubic perovskite oxide [32]. It is well known that bulk modulus is an indication of the resistant of the substance to compression. For the cubic system [15], bulk modulus can be evaluated from the equation below,

$$B = \frac{C_{11} + 2C_{12}}{3}$$
 (2)

The recorded value of bulk modulus using GGA and LDA functional were in line with the available literature [33]. Another important component corresponds to shear modulus which predicts the performance and capability of a material against distortions (shape deformation) diagonally. The shear modulus (G) was assessed by employing Voigt's(Gv) and the Reuss's (G<sub>R</sub>) approximations for the cubic system [34];

$$G_{V} = \frac{1}{r} \left( C_{11} - C_{12} + (3C_{44}) \right) \tag{3}$$

$$G_{V} = \frac{1}{5} (C_{11} - C_{12} + (3C_{44}))$$

$$C_{R} = \frac{5C_{44} \times (C_{11} - C_{12})}{4C_{44} + 3(C_{11} - C_{12})}$$
(3)
(4)

$$G = \frac{G_V + G_R}{2}$$
 (5)

Our findings as shown in Table 2 demonstrate that SrTiO<sub>3</sub> highly resist shape deformation suggesting that this compound is hard. Moreover, Yong modulus refers to another significant property of a material to withstand the elongation as a reference to the original length. It has been calculated from Equation 6;

$$E = \frac{9BG}{3B+G} \tag{6}$$

The Poisson's ratio (v) signifies the ratio of crosswise reduction tension to longitudinal

enlarging strain throughout stretching. Solid material typically exhibits Poisson's ratio ranging from 0.2-0.3. This ratio can be calculated from Equation 7.

Equation 7. 
$$v = \frac{3B - 2G}{6B + 2G}$$
 (7)

The Zener anisotropy factor (A) in solid is obtained from Equation 8 [35]. A material reveals isotropic property when A equals to unity. In contrast, higher or smaller values of A indicate that the material demonstrates anisotropy character. For cubic SrTiO<sub>3</sub>, A factor is reported to be less than 1, suggesting that SrTiO<sub>3</sub> is slightly anisotropy as recorded in Table 2.

$$A = \frac{2C_{44}}{C_{11} - C_{12}} \tag{8}$$

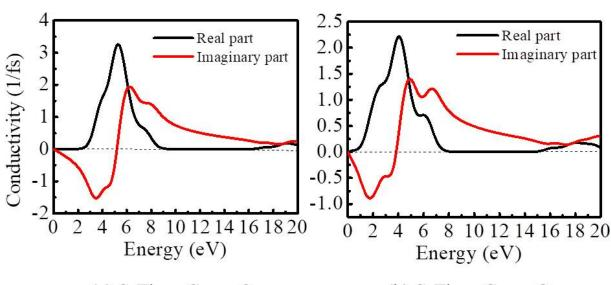
Finally, a measurement of material's brittleness or ductility can be evaluated through B/G value [36]. A material is considered ductile at high B/G value whereas, lower values indicate that the material is brittle. Moreover, the slandered value distinguish between ductility and brittleness correspond to 1.75. Based on this explanation, SrTiO<sub>3</sub> is predicted to be brittle.

## 4. CONCLUSIONS

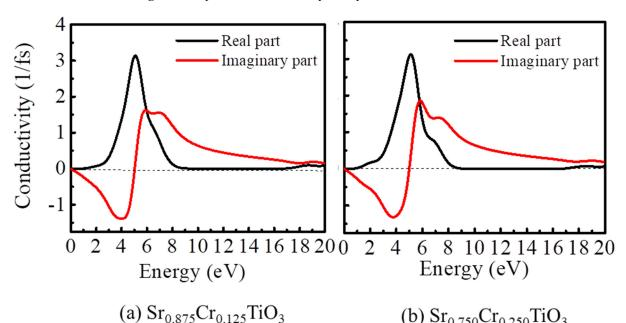
Strontium titanate (SrTiO<sub>3</sub>) is one of the perovskite materials having broad application in fields of optoelectronic industries.

This contribution provides an insight into ground state properties of pure SrTiO<sub>3</sub> including electronic, structure, optical, and mechanical characteristics via the state of art of firstprinciples calculations. Accordingly, the impact of Cr<sup>3+</sup> cation doping levels at the Sr and Ti sites of SrTiO<sub>3</sub> on the electronic structures and optical properties was investigated. Our simulated results revealed an agreement available experiment and predicted findings. Moreover, an adjustments on the electronic and optical properties was recorded after inserting Cr3+. Electronic band gap disappeared when Cr3+ atoms were located at Ti bulk site, transferring the material from semiconductor into conductive material, and metallic behavior. This behavior is confirmed by the literature that stated Cr3+ doping induces a transition from insulator/semiconductor to metal. In case of Cr<sup>3+</sup> inserted into and occupied Sr positions, the host system retained its semiconducting character, but with a gap energy on the visible region.





(b)  $SrTi_{0.750}Cr_{0.250}O_3$ (a)  $SrTi_{0.875}Cr_{0.125}O_3$ Fig. 13. The predicted conductivity of doped Cr-SrTiO<sub>3</sub> at Ti sites.



(b)  $Sr_{0.750}Cr_{0.250}TiO_3$ Fig. 14. The predicted conductivity of doped Cr-SrTiO<sub>3</sub> at Sr sites.

A comprehensive investigation of optical characteristics such as reflectivity, absorption, dielectric function and conductivity of the pure and Cr inserted SrTiO<sub>3</sub> enable us to reach a conclusion that the visible light absorption is improved by Cr3+ doping content. Such an outcome would support developing and designing new optoelectronics.

#### REFERENCES

Grabowska, E., "Selected Perovskite [1].

- Oxides: Characterization, Preparation and Photocatalytic Properties-A Review". Appl. Catal. B. 2016, 186, 97-126.
- [2]. A. Bera, K. Wu, A. Sheikh, E. Alarousu, O. F. Mohammed, and T. Wu, "Perovskite Oxide SrTiO<sub>3</sub> as an Efficient Electron Transporter for Hybrid Perovskite Solar Cells" J. Phys. Chem. C , 2014,118, 28494-28501.
- D. G. Schlom, L. Q. Chen, X. Pan, A. Schmehl, and M. A. Zurbuchen, "A Thin Film Approach to Engineering



- Functionality into Oxides", J. Am. Ceram. Soc. 2008, 91, 2429.
- [4]. F. Lo Presti, A. L. Pellegrino, and G. Malandrino, "Metal-Organic Chemical Vapor Deposition of Oxide Perovskite Films: A Facile Route to Complex Functional Systems", Adv. Mater. Interfaces 2022, 9, 2102501.
- [5]. M. Miyauchi, M. Takashio, and H. Tobimatsu, "Photocatalytic Activity of SrTiO<sub>3</sub> Codoped with Nitrogen and Lanthanum under Visible Light Illumination", Langmuir, 2004, 20, 232.
- [6]. R. Konta, T. Ishii, H. Kato, and A. Kudo, "Photocatalytic Activities of Noble Metal Ion Doped SrTiO<sub>3</sub> under Visible Light Irradiation", J. Phys. Chem. B, 2004,108, 8992.
- [7]. Y. Li, Q. Y. Hou, X. H. Wang, H. J. Kang, X. Yaer, J. B. Li, T. M. Wang, L. Miao, and J. Wang, "First-Principles Calculations and High Thermoelectric Performance of La-Nb Doped SrTiO<sub>3</sub> Ceramics", J. Mater. Chem. A 2019, 7, 236.
- [8]. B. Modak, "An Efficient Strategy to Enhance the Photocatalytic Activity of Ir-Doped SrTiO<sub>3</sub>: A Hybrid DFT Approach", New J. Chem. 2022, 46, 1507.
- [9]. P. Mei, J. Xiao, X. Huang, A. Ishag, and Y. Sun, "Enhanced Photocatalytic Reduction of U(VI) on SrTiO<sub>3</sub>/ g-C<sub>3</sub>N<sub>4</sub> Composites: Synergistic Interaction", Eur. J. Inorg. Chem. 2022, 2022, e202101005.
- [10]. J. W. Liu, G. Chen, Z. H. Li, and Z. G. Zhang, "Electronic Structure and Visible Light Photocatalysis Water Splitting Property of Chromium-Doped SrTiO<sub>3</sub>", J. Solid State Chem. 2006, 179, 3704.
- [11]. C. H. Chang and Y. H. Shen, "Synthesis and Characterization of Chromium Doped SrTiO<sub>3</sub> Photocatalyst", Mater. Lett. 2006, 60, 129.
- [12]. S. Tonda, S. Kumar, O. Anjaneyulu, and V. Shanker, Synthesis of Cr and La-Codoped SrTiO<sub>3</sub> Nanoparticles for Enhanced Photocatalytic Performance under Sunlight Irradiation, Phys. Chem. Chem. Phys. 16, 23819 (2014).
- [13]. H. A. Miran, Z. N. Jaf, M. Altarawneh, and Z. T. Jiang, An Insight into Geometries and Catalytic Applications of Ceo<sub>2</sub> from a Dft Outlook, Molecules 26, 6485 (2021).

- [14]. H. A. Miran, M. Altarawneh, Z. N. Jaf, B. Z. Dlugogorski, and Z. T. Jiang, "Structural, Electronic and Thermodynamic Properties of Bulk and Surfaces of Terbium Dioxide (TbO<sub>2</sub>)", Mater. Res. Express, 2018, 5, 085901.
- [15]. H. A. Miran, M. Altarawneh, H. Widjaja, Z. N. Jaf, M. Mahbubur Rahman, J. P. Veder, B. Z. Dlugogorski, and Z. T. Jiang, "Thermo-Mechanical Properties of Cubic Lanthanide Oxides", Thin Solid Films 2018, 653, 37.
- [16]. L. Triggiani, A. B. Muñoz-García, A. Agostiano, and M. Pavone, "Promoting Oxygen Vacancy Formation and P-Type Conductivity in SrTiO<sub>3</sub>: Via Alkali Metal Doping: A First Principles Study", Phys. Chem. Chem. Phys. 2016, 18, 28951.
- [17]. W. Wei, Y. Dai, H. Jin, and B. Huang, "Density Functional Characterization of the Electronic Structure and Optical Properties of Cr-Doped SrTiO<sub>3</sub>", J. Phys.D. Appl. Phys. 2009, 42, 055401.
- [18]. P. Reunchan, N. Umezawa, S. Ouyang, and J. Ye, "Mechanism of Photocatalytic Activities in Cr-Doped SrTiO<sub>3</sub> under Visible-Light Irradiation: An Insight from Hybrid Density-Functional Calculations", Phys. Chem. Chem. Phys. 2012, 14, 1876
- [19]. S. A. Azevedo, J. A.S. Laranjeira, J. L.P. Ururi, E. Longo, and J. R. Sambrano, "An Accurate Computational Model to Study the Ag-Doping Effect on SrTiO3", Comput. Mater. Sci., 2022, 214, 111693.
- [20]. E. Zhou, J.-M. Raulot, H. Xu, H. Hao, Z. Shen, and H. Liu, "Structural, Electronic, and Optical Properties of Rare-Earth-Doped SrTiO<sub>3</sub> Perovskite: A First-Principles Study". Phys. B Condens. Matter. 2022, 643, 414160.
- [21]. J. P. Perdew, K. Burke, and M. Ernzerhof, "Generalized Gradient Approximation Made Simple", Phys. Rev. Lett. 1996, 77, 3865.
- [22]. H. Widjaja, H. A. Miran, M. Altarawneh, I. Oluwoye, H. N. Lim, N. M. Huang, Z. T. Jiang, and B. Z. Dlugogorski, "DFT+ U and Ab Initio Atomistic Thermodynamics Approache for Mixed Transitional Metallic Oxides: A Case Study of CoCu<sub>2</sub>O<sub>3</sub> Surface Terminations", Mater. Chem. Phys. 2017, 201, 241.



- [23]. H. J. Monkhorst and J. D. Pack," Special Points for Brillouin-Zone Integrations", Phys. Rev. B 1976, 13, 5188.
- [24]. H. A. Miran and Z. N. Jaf, "Electronic and Optical Properties of Nickel-Doped Ceria: A Computational Modelling Study", Pap. Phys. 2022, 14, 140002.
- [25]. D. de Ligny and P. Richet, High-Temperature Heat Capacity and Thermal Expansion of and Perovskites, Phys. Rev. B - Condens. Matter. Mater. Phys. 1996, 53, 3013.
- [26]. S. Piskunov, E. Heifets, R. I. Eglitis, and G. Borstel, "Bulk Properties and Electronic Structure of SrTiO<sub>3</sub>, BaTiO<sub>3</sub>, PbTiO<sub>3</sub> Perovskites: An Ab Initio HF/DFT Study", Comput. Mater. Sci. 2004, 29, 165.
- [27]. Y. A. Abramov, V. G. Tsirelson, V. E. Zavodnik, S. A. Ivanov, and I. D. Brown, and "The Chemical Bond Atomic Displacements in SrTiO<sub>3</sub> from X-ray Diffraction Analysis", Acta Crystallogr. Sect. B 1995, 51, 942.
- [28]. K. Van Benthem, C. Elsässer, and R. H. French, "Bulk Electronic Structure of SrTiO<sub>3</sub>: Experiment and Theory", J. Appl. Phys. 2001, 90, 6156.
- [29]. G. I. Meijer, U. Staub, M. Janousch, S. L. Johnson, B. Delley, and T. Neisius, "Valence States of Cr and the Insulator-to-Metal Transition in Cr-Doped SrTiO<sub>3</sub>" Phys. Rev. B - Condens.Mater. Phys.2005, 72, 155102.
- [30]. Z. N. Jaf, Z. T. Jiang, H. A. Miran, and M. Altarawneh, "Thermo-Elastic and Optical Properties of Molybdenum Nitride", Can. J. Phys.2016, 94, 902 (2016).
- [31]. Z. N. Jaf, Z. T. Jiang, H. A. Miran, M. Altarawneh, J. P. Veder, M. Minakshi, Z. feng Zhou, H. N. Lim, N. M. Huang, and B. Z. Dlugogorski, "Physico-Chemical Properties of CrMoN Coatings - Combined Experimental and Computational Studies", Thin Solid Films 2020, 693, 137671.
- [32]. N. Pandech, K. Sarasamak, and S. Limpijumnong, "Elastic Properties of Perovskite A TiO<sub>3</sub> (A= Be, Mg, Ca, Sr, and Ba) and PbBO<sub>3</sub> (B= Ti, Zr, and Hf): First Principles Calculation"s, J. Appl. Phys. 2015, 117, 174108.
- [33]. A. A. Adewale, A. Chik, T. Adam, O. K. Yusuff, S. A. Ayinde, and Y. K. Sanusi,

- "First Principles Calculations of Structural, Electronic, Mechanical and Thermoelectric Properties of Cubic ATiO<sub>3</sub> (A= Be, Mg, Ca, Sr and Ba) Perovskite Oxide", Comput. Condens. Matter, 2021, 28, e00562.
- [34]. R. Hill, "The Elastic Behaviour of a Crystalline Aggregate", Proc. Phys. Soc. Sect. A 1952, 65, 349.
- [35]. C. Zener, Elasticity and Anelasticity of Metals (University of Chicago Press, Chicago Illinois, 1948.
- [36]. S. F. Pugh, XCII. "Relations between the Elastic Moduli and the Plastic Properties of Polycrystalline Pure Metals", London, Edinburgh, Dublin Philos. Mag. J. Sci. 1954, 45, 823.
- [37]. G. J. Fischer, Z. Wang, and S. ichiro Karato," Elasticity of CaTiO<sub>3</sub>, SrTiO<sub>3</sub> and BaTiO<sub>3</sub> Perovskites up to 3.0 Gpa: The Effect of Crystallographic Structure". Phys. Chem. Miner. 1993, 20, 97.



12

